Transp Porous Med (2008) 73:319–332
DOI 10.1007/s11242-007-9172-x

Analysis of Pore Network in Three-dimensional (3D) Grain Bulks Using X-ray CT Images

Sureshraja Neethirajan · Digvir S. Jayas

Received: 30 July 2006 / Accepted: 25 September 2007 / Published online: 23 October 2007

Abstract The knowledge of distribution of pore space inside grain bulks is essential for determining the airflow resistance of grains. In this study, the internal pore structure and the 3D-distribution of air paths inside grain bulks were studied using X-ray computed tomography images. Image analysis methods were applied to the binary 3D X-ray CT images on the spatial distribution of voids to generate the connected, individualized pore objects of different size and shapes. Morphometric parameters, such as 3D air path volume distribution, structure separation factor, Euler number, fragmentation index, and structure model index were calculated based on hexahedral marching cubes volume model and marching cubes 3D surface construction algorithm. The quantified numerical measures of spatial integrity of air path networks were analyzed and compared with the airflow resistance of grain bulks. The results showed that the connectivity of airspace and the nonuniform distribution of air-path network inside grain bulks were responsible for the difference in airflow resistance between horizontal and vertical directions to the airflow of grain bulks.

Keywords Pore network · Airflow resistance · Grain bulks · 3D image analysis · X-ray CT · Connectivity

1 Introduction

The value of Canada's annual grain crop is about CDN $6 billion and 70% of the produced grains are exported to global markets (Agriculture and Agri-Food Canada 2005). Fundamental and applied research on stored grains are essential for preserving harvested grains, to provide wholesome food, free of insect damage, and micro flora.

S. Neethirajan
The Canadian Wheat Board Centre for Grain Storage Research, Biosystems Engineering, University of Manitoba, Winnipeg, MB, Canada R3T 5V6

D. S. Jayas (✉)
University of Manitoba, 207 Administration Building, Winnipeg, MB, Canada R3T 2N2
e-mail: digvir_jayas@umanitoba.ca

Grains stored at moisture contents considered safe, may spoil because of moisture migration associated with inter-seed air currents (Acasio 1997). The rate of heat transfer through the grain bulk is different from that through the interstitial air surrounding the grain (Antic and Hill 2000). Air paths inside grain bulks are important criteria in estimating the time required for excess moisture to be removed during drying (Brooker 1961). In a study, Berck (1975) determined that interstitial air speed in grain bulk is influenced by the nature of the stored product, geometrical shape of the kernels, pore space and storage temperature.

Experimental techniques are needed for more reliable observation concerning the interior of the bulk of granular solid in designing the grain silos (Nielsen 1998). Giner and Denisienia (1996), while determining pressure drop through wheat bulk, emphasized that models should be developed to relate the pressure drop with void fraction and particle diameter.

Ergun's equation, (Smith 1996) the most commonly used equation for calculating airflow resistance in grain during drying in grain bins includes the influence of void fraction (pore space) and particle diameter. Permeability is an important material property in determining the magnitude of natural convection currents during periods of non-aerated storage. Fluid transport models developed by researchers in soil science and rock geometry prove that there is a functional relationship between transport coefficients and pore geometrical characteristics. According to Poiseuille's law, local hydraulic conductivity is dependent on the dimensions of the pore.

$$K(R, L) = \frac{\pi R^4}{8\mu L}$$

where K = hydraulic conductivity ($m^3\ s^{-1}\ Pa^{-1}$), R = aperture of the pore (m), L = length of pore space (m), μ = viscosity of air (Pa.s).

By calculating the local conductivity associated with each pore, overall permeability of airflow inside grain bulks can be determined. In grain storage, researchers have not developed any fluid transport models linking conductivity parameters to pore space geometry and pore-size distribution. In order to gain confidence in the models predicting conductivity, future research is needed for measuring conductivity parameters to link the pore space geometry. The geometry of the pore structure inside grain bulks will be useful in developing and validating mathematical models of grain drying and aeration. The pore topology inside the grain bulks will help to predict the air traverse time and the cooling or fumigation pattern which in turn are essential for the design of storage management strategies (Smith and Jayas 2004; Smith et al. 2001). In addition, the inter-granular pore network will enhance our understanding of the mechanism of packing of grains inside the silos. Hence, there is a need to quantify and develop the structural parameters of air paths inside grain bulks.

The resistance to airflow through grains is affected by several factors, such as air velocity, viscosity, grain surface roughness characteristics, and configuration of voids. Jayas et al. (1987) conducted experiments to determine the effect of these parameters on the resistance of airflow in grains and determined that there is a difference in airflow resistance between horizontal and vertical directions in seed bulks. They concluded that the orientation of particles and the differential void space distribution in both directions might have contributed to the difference in airflow resistance. Kay et al. (1989) while studying the horizontal and vertical airflow resistance of corn speculated that the differences in air pathway sizes and lengths might have caused the airflow resistance differences. It will be possible to completely calculate the velocity field of fluid flow within a bulk of grains provided the geometry of the interphase boundaries be quantified and specified (Hood and Thorpe 1992). Theoretical investigations of Endo et al. (2002) showed that particle heterogeneity, pore size distribution

and pore shape significantly influence permeation resistance of gas through a granular packed bed. Until now, no scientific effort has been made to explain the reason behind the difference in airflow resistances along both the directions of grain bulk, because no suitable techniques have been available. The quantification and analysis of pore network topology will help to explain this difference and in understanding the effect of porosity on the airflow resistance of grains.

The inherent heterogeneity of porous media and the complexity involved in quantifying the air path network and the pore morphology inside the grain bulk is a significant challenge. Recent advances in imaging methods and the computational capability have resulted in the ability to measure parameters, which were otherwise impossible. X-ray computed tomography (CT) could reliably describe the pore structure and connectivity of real samples (Turners et al. 2003). Significant research has been done to analyze the pore network using tomography images in soil cores and water flow in porous media (Lindquist, 2002; Kainourgiakis et al. 2005). A micro-CT scan followed by 3D reconstruction of serial image sections can determine porosity, pore size, pore interconnectivity, strut size, and overall 3D micro architecture (Darling and Sun 2004).

Therefore, the objectives of this study were:

(i) to generate and characterize air path networks inside grain bulks from the X-ray CT images and
(ii) to quantify pore geometry and correlations that occur at the pore scale inside the grain bulks using image-processing techniques on the X-ray CT images.

2 Materials and Methods

2.1 Samples

Five types of grains were selected for CT scanning based on their shape to give potentially different airflow paths. These were hard red winter wheat (referred to as wheat, hereinafter), barley, flax seed, peas, and mustard. Out of these samples, wheat and barley are oblong and ellipsoidal in shape, flax seed is also oblong, but similar to the shape of a flattened speedboat, and peas and mustard are almost spherical. All the grain samples were further sifted manually to remove stone, straw and chaff particles. The resolution of the X-ray CT image depends on the size of the sample. For smaller seeds like flax seed and mustard, the resolution of the image must be high to get a clear image. Hence, two sizes of sample containers were used for scanning. Clean grain samples of wheat, peas, and barley were filled from a height of 20 cm from the top of the container in three separate 15-cm side cubic containers made of optically transparent acrylic, while flax seed and mustard were filled in two, 7.5 cm side cubic containers. Filling procedure affects the bulk density and the packing structure of the granular airspace inside the grain bulks. Grain kernels tend to orient themselves with their longer axis in a plane normal to the gravitational field. In North America, mechanical spreaders are used to distribute foreign material to improve airflow through the grain resulting in nearly leveled grain surface and compaction of grain. In our study, after the samples were filled in the container, they were shaken well for compaction. The measured air path and the pore space features inside grain bulks include the condition of packed grain bulk at compaction. The containers were sealed tightly by placing cotton on the top of the compact grain bulk with a lid to avoid the change in orientation of kernels while scanning. The packed bed height was 15 cm for wheat, barley, and peas bulks, and 7.5 cm for flax seed and mustard

Table 1 Physical properties of grain samples

Grain type	Moisture content (%)	Length (mm)	Width (mm)	Thickness (mm)	Mass of 1000 seeds (g)
Wheat	12.1	5.5 ± 0.79	2.8 ± 0.15	2.9 ± 0.14	39.2
Barley	11.2	9.4 ± 1.01	3.6 ± 0.25	2.4 ± 0.18	36.1
Flax seed	8	4.2 ± 0.51	2.3 ± 0.10	0.9 ± 0.15	6.8
Peas	11.5	7.9 ± 0.23	7.2 ± 0.20	6.7 ± 0.15	279
Mustard	8.1	2.5 ± 0.12	2.3 ± 0.10	2.3 ± 0.10	8.9

Standard deviation at $N = 1{,}000$

Table 2 Summary of image characteristics of different grain bulks

Grain type	Image resolution μm	Slice thickness (mm)	Number of slices	Image size for analysis (pixel × pixel)	Image size for analysis (cm × cm)
Wheat	200	0.25	200	667 × 667	14.3 × 14.3
Barley	200	0.25	200	667 × 667	14.3 × 14.3
Flax seed	120	0.125	350	631 × 631	7.0 × 7.0
Peas	200	0.25	200	667 × 667	14.3 × 14.3
Mustard	120	0.125	350	631 × 631	7.0 × 7.0

bulk samples. The physical properties of the grain samples and the measured mean values of grain dimensions are shown in Table 1.

2.2 Imaging of Samples

The X-ray CT images of all grain samples were scanned using a Bio-imaging Research X-ray CT scanner at University of Texas, Austin. The samples were scanned only at the middle of the container for a 50-mm thickness for both the horizontal and vertical directions representing perpendicular and parallel pore spaces, respectively, to the direction of filling the container. There were totally 2,600 images, 200 images in each direction of scanning for wheat, barley and peas bulk while 350 images in each direction of scanning for mustard and flax seed bulk. All original images were of 1,024 × 1,024 pixels sizes, which were cropped to extract region of interest for further analysis (Table 2).

2.3 Pre-Processing of the 3D X-Ray Data

Algorithms developed by CT Analyser (version 1.4, Skyscan, Belgium) were used for preprocessing and morphometric feature extraction of voids inside the grain bulk image. The spatial boundary between voids and the grain were established due to the difference in densities from the X-ray CT images. The images were thresholded using Otsu's adaptive technique (Yang et al. 1996) to separate air space and grain. The X-ray CT images were preprocessed using the following steps to facilitate pore geometry analysis (Figs. 1,2):

(1) Image cropping for the region of interest (Table 2);
(2) adaptive thresholding to obtain the binary processed image;
(3) 3D Reconstruction for volume model of X-ray data; and

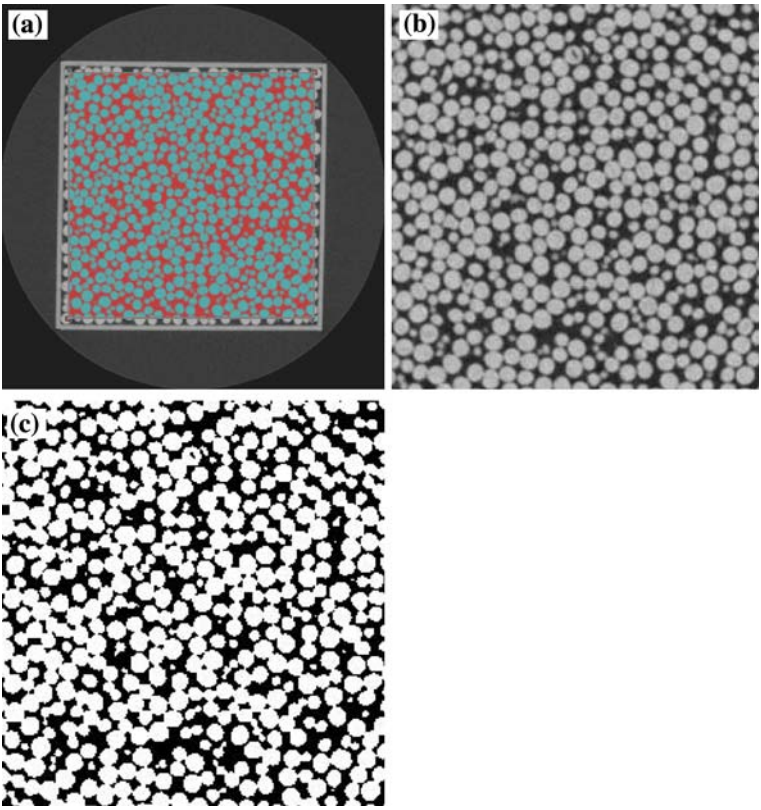

Fig. 1 X-ray CT images of peas bulk. (**a**) Original X-ray CT image, (**b**) cropped image, (**c**) thresholded image

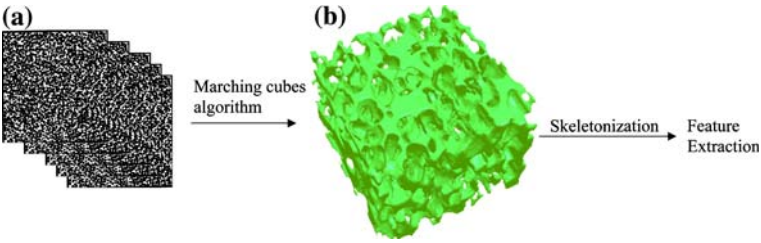

Fig. 2 Pre-processing of the 3D X-ray data (**a**) Serial stack of thresholded X-ray CT images, (**b**) Reconstructed cut section of the 3D volume model for peas bulk

(4) Skeletonization and feature extraction.

2.4 Structural Parameters Extraction

The pore structure inside grain bulks has to be characterized by parameters that will explain the fundamental relationship among architecture, geometry of pore topology, and the spatial continuity of the network with the transport phenomena. As the pore space network models are intended to provide predictions of permeability and hydraulic conductivity properties, the

Table 3 Comparison of calculated bulk densities of grain samples with the reported values

Grain type	Calculated bulk density (kg/m^3)	Reported bulk density (kg/m^3)
Wheat	760	772 (Kumar and Muir 1986)
Barley	603	610 (Kumar and Muir 1986)
Flax seed	637	642 (Irvine et al. 1992)
Peas	375	379 (Alagusundaram et al. 1992)
Mustard	684	690 (Velasco et al. 1998)

geometry of the pore network has to be adapted to relevant observable parameters of the pore space structure. Minkowski functionals (Mecke 1998) characterize connectivity, content and shape of pore space through integral geometric approach. Minkowski functionals include measures such as Euler characteristics, volume, and integral of mean curvature (concavity or convexity of surface). Euler number and fragmentation index are numerical measures and are effective indices of spatial integrity (Bogaert et al. 2002). From the X-ray CT images of grain bulks, Euler characteristic and fragmentation index were determined and used as a measure of connectivity. The other morphometric parameters such as 3D air path volume distribution, structure separation and structure model index, were also calculated in 3D from the hexahedral marching cubes volume model and marching cubes 3D surface construction algorithms (Bouvier 1997; Feldcamp et al. 1984; Lorensen and Cline 1987).

All the grain sample images were analyzed using image processing techniques and morphometric structural parameters for each grain bulk were extracted for both the horizontal and vertical directions. An independent group *t*-test was done to check the difference between the means of the morphometric parameters in both the horizontal and vertical directions for all grains (SAS version 8.2, Statistical Analysis Systems, Cary, NC).

3 Results and Discussion

3.1 Bulk Density

Table 3 compares the bulk densities measured from the samples and the reported bulk densities in the literature. Based on these data, it was assumed that the grain samples used for this study reasonably represented the bulk grain.

3.2 Morphometric Parameters Analysis

3.2.1 Euler Number (Eu.N)

Euler number is an indicator of connectedness of a 3D complex pore space and a global characterization of topology (Vogel et al. 2002). Vogel and Babel (1996) showed how to get an estimation of Euler characteristic from a cubic packing of spheres. In our study, the mathematical morphological functions such as erosion and dilation were applied using the algorithms on the 3D reconstructed model of the pore space to get a measure of the Euler number. It measures redundant connectivity, the degree to which parts of the object are multi-connected (Odgaard and Gundersen 1993). The Euler–Poincare formula for a 3D object is:

$$\text{Eu.N} = \beta_0 - \beta_1 + \beta_2 \tag{1}$$

where β_0 is the number of objects, β_1 is the connectivity and β_2 is the number of enclosed cavities. Euler analysis provides a measure of connectivity density indicating the number of redundant connections between void (air path) structures per unit volume. Euler number is related to the total volume of the sample. Euler number is positive or has a higher value when the number of isolated pores that are not connected to each other that exceeds the number of multiple connections between the pores. The Euler number is negative or has a lower value for a completely connected network of pores in which case it counts the number of multiple connections and corresponds to the number of meshes in the pore network. In short, Euler characteristic is a measure of connectivity which gives higher values for poorly connected structures and lower values for better-connected structures.

Euler number increases from slice 1 to slice 200 in the vertical direction of wheat and barley seed bulk indicating increase of inter nodal air paths and poor connectivity of air paths from the bottom to top of these grain bulks (Fig. 3). The poorer connectivity along the vertical airflow direction may resist the air to pass through. But in the horizontal direction of wheat and barley seed bulks, almost same amount of inter nodal air paths are present from slice 1 to slice 200 representing similar connectivity of air paths along the direction of air flow. The airflow resistance ratio between horizontal and vertical direction for wheat and barley seed bulk are 0.63 and 0.47 (Kumar and Muir 1986), respectively. The mean Euler number ratio between vertical to horizontal direction for wheat and barley seed bulk are 0.66 and 0.48 respectively. There is no significant difference in Euler numbers between the horizontal and vertical direction of the peas bulk. The airflow resistance is same in both the horizontal and vertical directions of peas bulk (Alagusundaram et al. 1992) which may be explained by the same number of inter nodal structures and similar connectivity in both the horizontal and vertical direction.

In the flax seed bulk, the Euler number decreases from slice 1 to slice 200 and then it increases from slice 200 to slice 350. The mean Euler number ratio between vertical to horizontal direction for flax seed bulk is 1.9 which is not equivalent to 0.49 (Jayas et al. 1991), the airflow resistance ratio between horizontal to vertical direction of flax seed. The mean Euler number ratio between horizontal to vertical direction for mustard bulk is 1.07 which is not equivalent to 0.78 (Velasco et al. 1998). Euler number can potentially explain the difference in airflow resistances along the horizontal and vertical directions of the bulks for wheat, barley and peas, but not for flax seed and mustard grain bulk.

3.2.2 Fragmentation Index (Fr.I)

Fragmentation index is an index of connectivity of air paths. Hahn et al. (1992) calculated an index of relative convexity or concavity of the total surface, on the principle that concavity indicates connectivity (and the presence of nodes) and, convexity indicates isolated disconnected structures (struts). Fr.I is calculated in 3D, by comparing area and perimeter (or volume and surface, respectively) of binarized solid before and after an image dilation.

$$\text{Fr.I} = \left(\frac{P_1 - P_2}{A_1 - A_2}\right) \tag{2}$$

Where P and A are solid area and perimeter, and the subscript numbers 1 and 2 indicate before and after image dilation. Lower fragmentation index signifies better connected lattices while the higher value of Fr.I indicates more disconnected void (air path) structures.

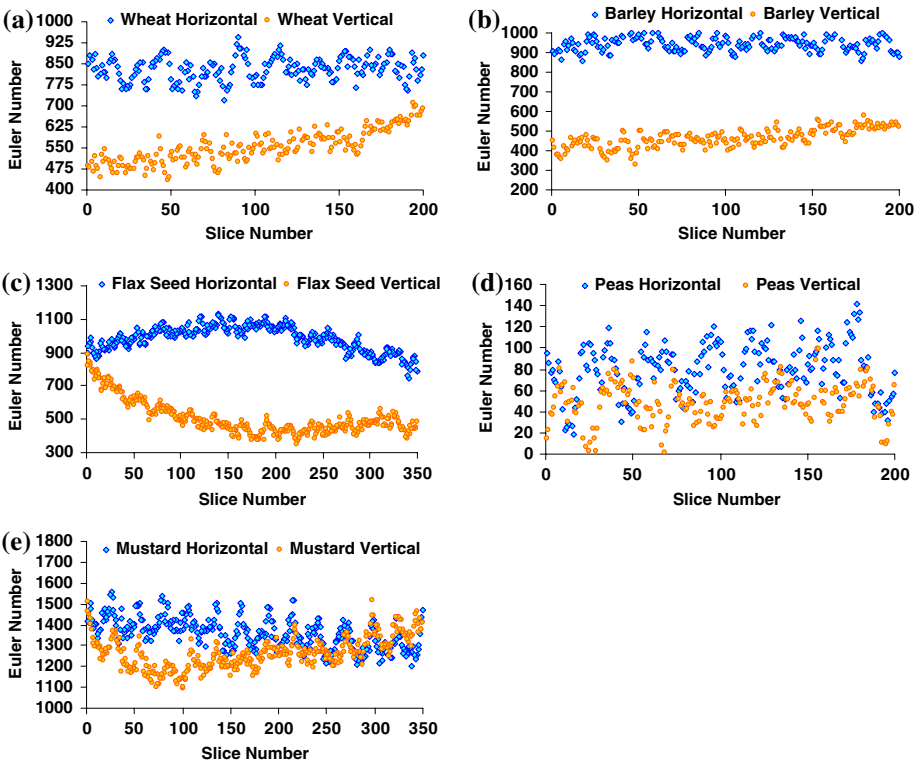

Fig. 3 Euler number distribution for (**a**) wheat, (**b**) barley, (**c**) flax seed, (**d**) peas, (**e**) mustard seed bulks

There are more disconnected air paths in the horizontal direction of wheat, barley, and flax seed bulk (Fig. 4) than in the vertical direction. The fragmentation index increases from slice 1 to slice 200 in the vertical direction of wheat and barley seed bulk indicating an increase of disconnected air paths from bottom to the top of the grain bulk. In the horizontal direction of these grain bulks, almost same number of disconnected air paths is present for all slices. Same amount of disconnected air paths along the air flow direction (slices) may facilitate the air to pass through easily in the horizontal direction. The resistance offered to airflow in the vertical direction of wheat and barley seed bulk is higher because the number of better connected air path structures decreases from the bottom to top of the grain bulk. In the flax seed bulk, the fragmentation index decreases from slice 1 to slice 200 and it increases from slice 200 to slice 350.

There is no significant difference in fragmentation index between the horizontal and vertical direction of peas and mustard bulk. Well-connected air path network in both the horizontal and vertical directions of peas bulk results in similar airflow resistance in both the directions. Fragmentation index is the lowest for peas bulk indicating better connected air path network than the other seed bulks. Mustard seed bulk has more disconnected air paths than the rest of the seed bulks.

Unlike wheat and barley, fragmentation index and Euler number analyses in vertical direction of flax seed and mustard bulk decreases from slice 1 to slice 200 and increases from slice 201 to slice 350. This trend contradicts the fact that the grain bulk will have higher compaction at bottom than top. This may be due to the lower resolution of the X-ray CT

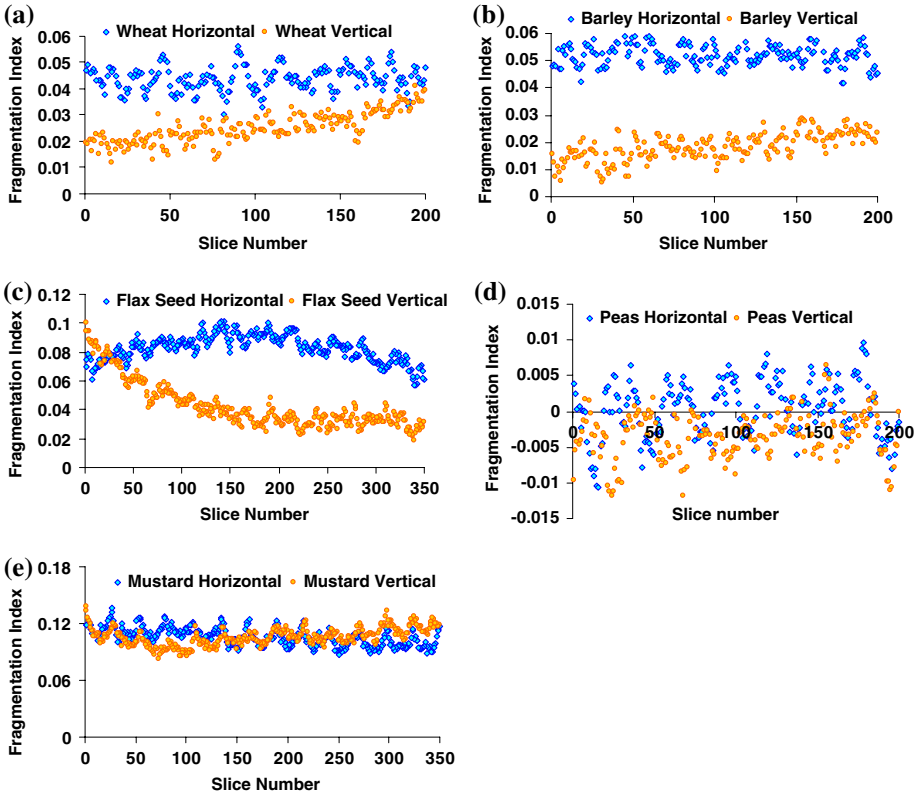

Fig. 4 Fragmentation index distribution for (**a**) wheat, (**b**) barley, (**c**) flax seed, (**d**) peas, (**e**) mustard seed bulks

images for smaller seeds such as flax seed and mustard. Future work is essential to analyze the smaller size seed bulk with high-resolution X-ray CT images.

3.2.3 3D Airpath Volume Distribution

Figure 5 shows the 3D air path volume distribution inside the grain bulks. An independent group t-test showed that the 3D air path volumes in both horizontal and vertical directions for wheat, barley, and flax seed grain bulks are statistically different ($P < 0.05$).

In wheat, barley, and flax seed bulk, the air path volumes are higher in horizontal direction than in the vertical direction. The air path volumes in the range of 0–128 pixels are higher inside wheat bulk than the peas bulk but a few number of larger air path volumes (128–512 pixel range) are present in peas bulk. This explains the higher airflow resistance of wheat (33 Pa/m) compared to the lower airflow resistance of peas bulk (4.5 Pa/m) at air velocity of 0.1 $m^3/(s\,m^2)$ (ASAE Standards 2003).

The absolute percentage difference in air path volumes between horizontal to vertical direction of wheat, barley and flax seed bulk ranges from 17 to 44%, 34 to 58%, and 22 to 64%, respectively. The difference in air path volumes between horizontal and vertical direction inside the grain bulks may explain the difference in airflow resistances in both the directions.

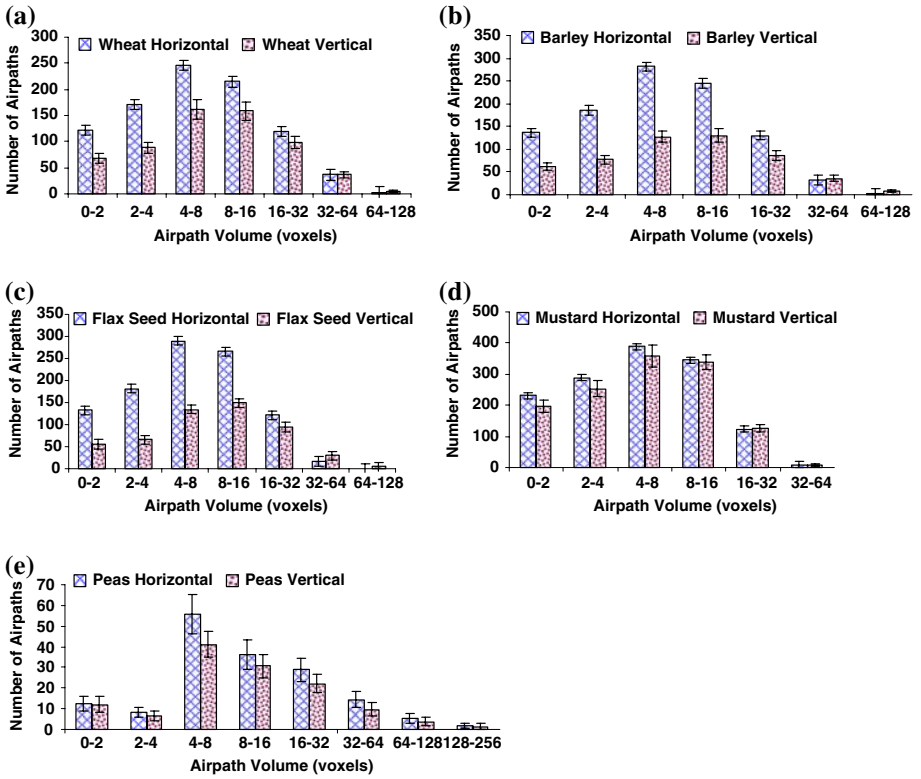

Fig. 5 3D air path volume distribution in (**a**) wheat, (**b**) barley, (**c**) flax seed, (**d**) peas, (**e**) mustard seed bulks

In peas and mustard seed bulks, there are no differences in air path volumes between the horizontal and vertical direction. Peas bulk offers similar resistance to airflow in both the horizontal and vertical directions which may be explained by the equal air path volume distribution in both the directions. The airflow resistance ratio between horizontal to vertical direction in mustard seed bulk is 0.72 (Velasco et al. 1998). Air paths with volumes larger than 64 voxels are present only inside peas bulk but not in the mustard bulk. There is more number of air paths with smaller volumes present inside mustard bulk than the peas bulk. Smaller seeds, such as mustard pack tighter and could create a higher static pressure than larger seeds like peas.

3.2.4 Structure Model Index (SMI)

In predicting permeability of airflow inside granular solid bulks and in determining the wetting phases and pore wall roughness, it is necessary to describe the shape of the pore space (Blunt 2001). Structure model index indicates the relative prevalence of rods and plates in a 3D structure. Structure Model Index involves a measurement of surface convexity. This parameter is of importance because it characterizes the transition from plate-like to rod-like architecture. An ideal plate, cylinder and sphere have SMI values of 0, 3 and 4, respectively. The calculation of SMI is based on dilation of the 3D voxel model by artificially adding one voxel thickness to all binarized object surfaces (Hildebrand and Ruegsegger 1997). SMI is defined as follows:

$$\mathrm{SMI} = 6X(S'XV/S^2) \tag{3}$$

Table 4 Structure model indices for grain samples

Grain	Direction of airflow	Structure Model Index (pixels)
Wheat	Horizontal	1.03
	Vertical	0.89
Barley	Horizontal	1.23
	Vertical	0.85
Flax seed	Horizontal	1.61
	Vertical	1.34
Peas	Horizontal	0.27
	Vertical	0.24
Mustard	Horizontal	1.84
	Vertical	1.82

where S is the object surface area before dilation and S' is the change in surface area caused by dilation. V is the initial, undiluted object volume.

The structure model indices in horizontal directions of all the grain bulks are higher than the vertical direction (Table 4). The values of SMI indicate that the air spaces in horizontal direction are towards a rod like architecture than the plate like architecture. Configuration of voids and orientation of particles may be responsible for airflow resistance differences between the horizontal and vertical directions of grain bulks (Jayas et al. 1987). In wheat, barley, flax seed and mustard bulks, the airflow resistance is lower in horizontal direction than in the vertical direction. Rod like architecture of air paths in horizontal direction may facilitate faster movement of air resulting in lower airflow resistance than in the vertical direction.

The shape of air spaces inside peas bulk is same in both the directions. This means that all the peas seeds were equally spaced among themselves during packing in both the horizontal and vertical directions to airflow, resulting in similar airflow resistances in both directions (Alagusundaram et al. 1992). The SMI value is lower for peas bulk than the other seed bulks.

3.2.5 Structure Separation (Sr.Sp)

Structure separation is essentially the thickness of the air paths as defined by binarization within the volume of interest in the grain bulk. Physically, this represents the diameter of a cylinder having volume and length equal to the volume and length of the airflow path. It is calculated three dimensionally from 2D images with cylinder rod model (Parfitt et al. 1987). Structure separation is calculated as:

$$\text{Sr.Sp} = \text{Sr.Th} \times \left(\left[\left(\frac{4}{\pi} \right) \times \left(\frac{TV}{SV} \right) \right] - 1 \right) \tag{4}$$

Where TV is the total volume of interest, SV is the solid (grain) volume, Sr.Th = 2/(Surface to Volume ratio).

Figure 6 shows the air path thickness distribution in wheat, barley and flax seed bulks. Air path thicknesses are same (not significantly different) in both the horizontal and vertical directions of wheat, barley and flax seed bulk. Wheat and barley bulk have same mean air

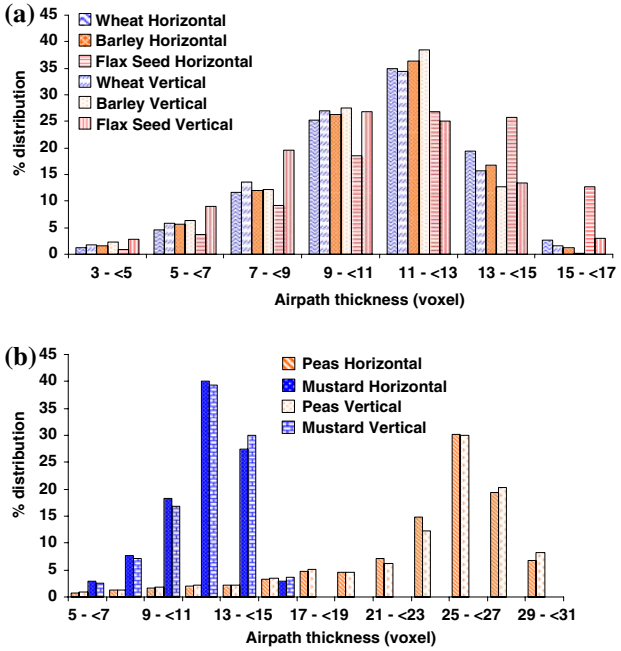

Fig. 6 Structure separation distribution in (**a**) Wheat, barley and flax seed bulk, (**b**) peas and mustard bulk

path thickness with 14.25 voxels in both the directions. The mean air path thicknesses in horizontal and vertical directions of flax seed bulk are 13.9 and 14.2 voxels, respectively.

There is no significant difference in air path thicknesses between the horizontal and vertical direction for peas and mustard bulk. Air path thicknesses are larger in peas bulk (>17 voxels) than in the mustard bulk. Airpath thickness (structure separation) do not aid in explaining the airflow resistance differences in both the directions of grain bulks.

4 Summary

Knowledge of the complex pore network topology inside grain bulks can be obtained by 3D volumetric X-ray CT image analyses of grains. 3D model generated from the X-ray CT images is a reliable and accurate method of determination of void space inside grain bulks. Techniques for the reconstruction of the void space inside grain bulks using X-ray CT images are described. Morphometric parameters measured on the 3D X-ray tomographic data using the image processing algorithms revealed information about the connectivity of the air path structure and allowed for the estimation of air path size distribution. The interconnectivity, the pore topology network measurements and the 3D air path volume distribution inside grain bulks explains the airflow resistance difference in both the directions of grain bulks. Future work is needed to analyze the smaller size seeds using X-ray CT images obtained with a scanner with high resolution.

Acknowledgements The authors gratefully acknowledge the Natural Sciences and Engineering Research Council of Canada and the Canada Research Chairs program for providing financial support for this project.

The authors also thank the Centre for Bone and Periodontal Research, Montreal, Canada for providing access to CT Analysis software for analysing the images.

References

Acasio, U.A.: Handling and Storage of Soybeans and Soybean Meal. American Soybean Association, St. Louis, MO (1997)

Agriculture and Agri-Food Canada: Agriculture: Food and Much more. Available at: http://www.agr.gc.ca/cb/brochure/cwb_e.phtml (2005/12/27). Accessed 26 December 2005

Alagusundaram, K., Jayas, D.S., Chotard, F., White, N.D.G.: Airflow pressure drop relationships of some specialty seeds. Sci. Des. Alim. **12**, 101–116 (1992)

Antic, A., Hill, J.M.: A mathematical model for heat transfer in grain store microclimates. Austr. NewZ. Indus. Appl. Math. J. **42**, 117–133 (2000)

ASAE Standard.: Resistance to airflow of grains, seeds, other agricultural products, and perforated metal sheets. ASAE D272.3 DEC01. American society of Agricultural Engineers, St. Joseph, MI (2003)

Berck, B.: Determination of air movement in stored grain as a factor of dynamic dispersion and distribution patterns of gaseous pesticides (fumigants). Bull. Environ. Contam. Toxic **13**, 527–533 (1975)

Blunt, M.J.: Flow in porous media—pore network models and multiphase flow. Curr. Opin. Colloid Interface Sci. **6**, 197–207 (2001)

Bogaert, J., Hecke, P.V., Ceulemans, R.: The Euler number as an index of spatial integrity of landscapes: evaluation and proposed improvement. Environ. Manage. **29**, 673–682 (2002)

Bouvier, D.J.: Double Time Cubes. A Fast 3D Surface Reconstruction Algorithm for Volume visualization. International Conference on Imaging, Science Systems and Technology, Las Vegas, Nevada (1997)

Brooker, D.B.: Pressure patterns in grain drying systems established by numerical methods. Trans. Am. Soc. Agric. Eng. **4**, 72–77 (1961)

Darling, A., Sun, W.: 3D Microtomographic characterization of precision extruded poly-ε-caprolactone tissue scaffolds. J. Biomed. Mater. Res. Appl. Biomater. **70**, 311–317 (2004)

Endo, Y., Chen, D., Pui, D.Y.H.: Theoretical consideration of permeation resistance of fluid through a particle packed layer. Power. Technol. **124**, 119–126 (2002)

Feldkamp, L.A., Davis, L.C., Kress, J.W.: Practical cone-beam algorithm. J. Opt. Soc. Am. **1**, 612–619 (1984)

Giner, S.A., Denisienia, E.: Pressure drop through wheat as affected by air velocity, moisture content and fines. J. Agric. Eng. Res. **63**, 73–86 (1996)

Hahn, M., Vogel, M., Pompesius-Kempa, M., Delling, G.: Trabecular bone pattern factor—a new parameter for simple quantification of bone microarchitecture. Bone **13**, 327–330 (1992)

Hildebrand, T., Ruegsegger, P.: Quantification of bone microarchitecture with the structure model index. Comp. Meth. Biomech. Biomed. Eng. **1**, 15–23 (1997)

Hood, T.J.A., Thorpe, G.R.: The effects of anisotropic resistance to air flow on the design of aeration systems for bulk stored grains. Agric. Eng. Aust. **21**, 18–23 (1992)

Irvine, D.A., Jayas, D.S., White, N.D.G., Britton, M.G.: Physical properties of flax seed, lentils, and fababeans. Can. Agric. Eng. **34**, 75–81 (1992)

Jayas, D.S., Alagusundaram, K., Irvine, D.A.: Resistance to airflow through bulk flax seed as affected by the moisture content, direction of airflow and foreign material. Can. Agric. Eng. **33**, 279–285 (1991)

Jayas, D.S., Sokhansanj, S., Moysey, E.B., Barber, E.M.: The effect of airflow direction on the resistance of canola (rapeseed) to airflow. Can. Agric. Eng. **29**, 189–192 (1987)

Kainourgiakis, M.E., Kikkinides, E.S., Galani, A., Charalambopoulou, G.C., Stubos, A.K.: Digitally reconstructed porous media: transport and sorption properties. Transp. Porous Media **58**, 43–62 (2005)

Kay, R.L., Bern, C.J., Hurburgh, C.R.: Horizontal and vertical airflow resistance of shelled corn at various bulk densities. Trans. Am. Soc. Agric. Eng. **32**, 733–736 (1989)

Kumar, A., Muir, W.E.: Airflow resistance of wheat and barley affected by airflow direction, filling method and dockage. Trans. Am. Soc. Agric. Eng. **29**, 1423–1426 (1986)

Lindquist, W.B.: Quantitative analysis of three dimensional X-ray tomographic images, in developments in X-ray Tomography III. In: Proceedings of SPIE, 4503, pp. 103–115. SPIE, Bellingham, USA, July 7–10 (2002)

Lorensen, W.E., Cline, H.E.: Marching cubes: a high resolution 3D surface construction algorithm. Comp. Graph **21**, 163–169 (1987)

Mecke, K.R.: Integral geometry and statistical physics. Int. J. Mod. Phy. B **12**, 861–899 (1998)

Nielsen, J.: Pressures from flowing granular solids in silos. Philos. Trans. R. Soc. Lond. A **356**, 2667–2684 (1998)

Odgaard, A., Gundersen, H.J.: Quantification of connectivity in cancellous bone, with special emphasis on 3-D reconstructions. Bone **14**, 173–182 (1993)

Parfitt, A.M., Drezner, M.K., Glorieux, F.H., Kanis, J.A., Malluche, H., Meunier, P.J., Ott, S.M., Recker, R.R.: Bone histomorphometry: standardization of nomenclature, symbols and units. J. Bone. Miner. Res. **2**, 595–610 (1987)

Smith, E.A.: Pressure and velocity of air during drying and storage of cereal grains. Transp. Porous Media **23**, 197–218 (1996)

Smith, E.A., Jayas, D.S.: Calculation and limitations of traverse time in designing forced ventilation systems. Trans. Am. Soc. Agric. Eng. **47**, 1635–1642 (2004)

Smith, E.A., Jayas, D.S., Ville, A.de : Modelling the flow of carbon dioxide through beds of cereal grains. Trans. Porous Media **44**, 123–144 (2001)

Turner, M., Sakellariou, A., Arns, C., Sok, R., Limaye, A., Sendent, T. and Knacksted, M.: Towards Modelling Regolith Permeability with High Resolution X-ray Tomography. Adv. Rego., CRC LEME, Adelaide, Australia (2003)

Velasco, L., Jose, M.M., Haro, A.: Application of near-infrared reflectance spectroscopy to estimate the bulk density of ethiopian mustard seeds. J. Sci. Food. Agric. **77**, 312–318 (1998)

Vogel, H.J., Babel, U.: Topological characterization of pore space in soil-sample preparation and digital image processing. Geoder **73**, 23–28 (1996)

Vogel, H.J., Cousin, I., Roth, K.: Quantification of pore structure and gas diffusion as a function of scale. Euro. J. Soil. Sci. **53**, 465–473 (2002)

Yang, C., Chung, P., Chang, C.: Hierarchial fast two dimensional entropy thresholding algorithm using a histogram pyramid. Opt. Eng. **35**, 3227–3241 (1996)